

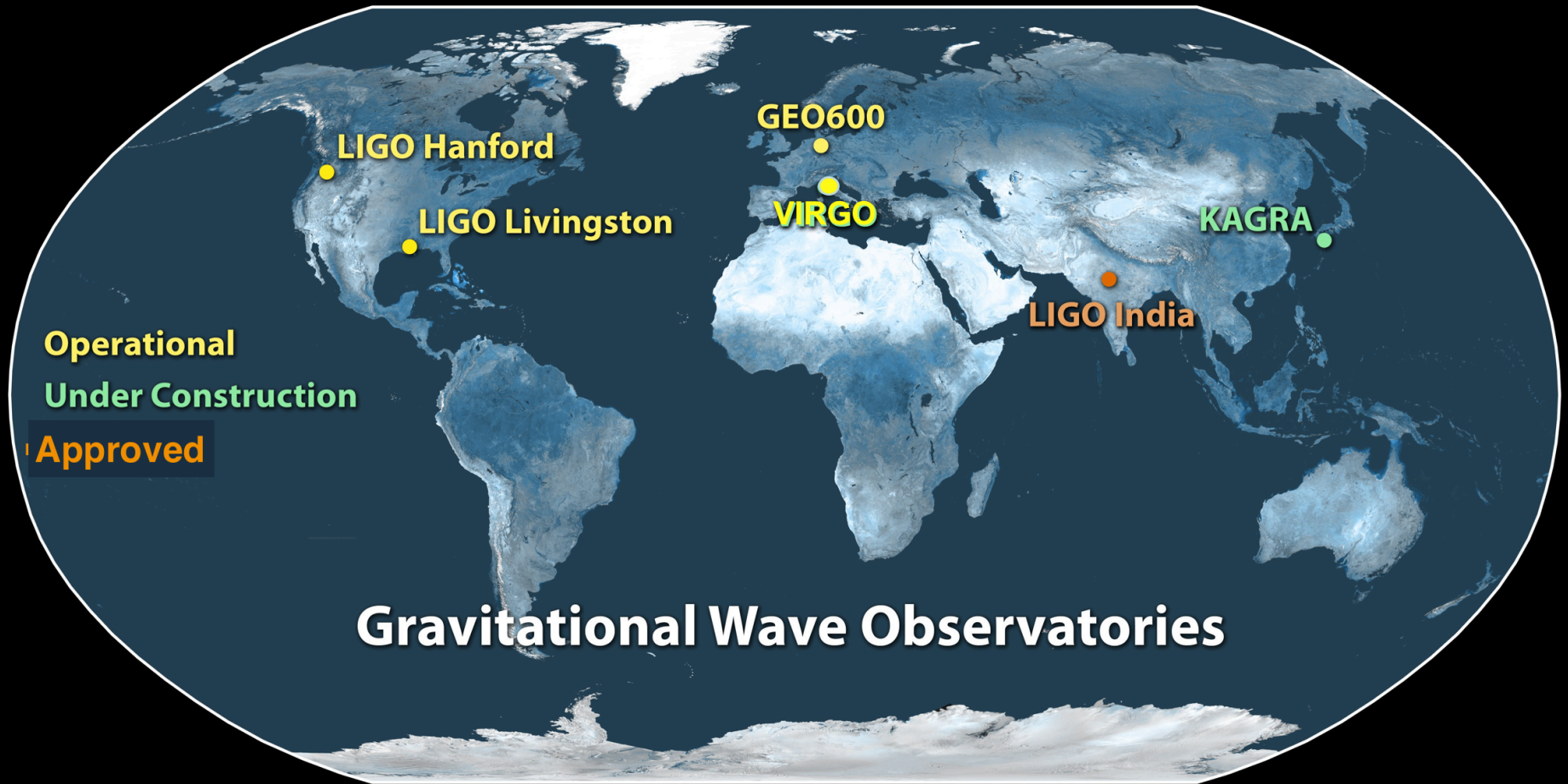


Advanced Virgo: the present and future challenges

Cristiano Palomba (INFN Roma)

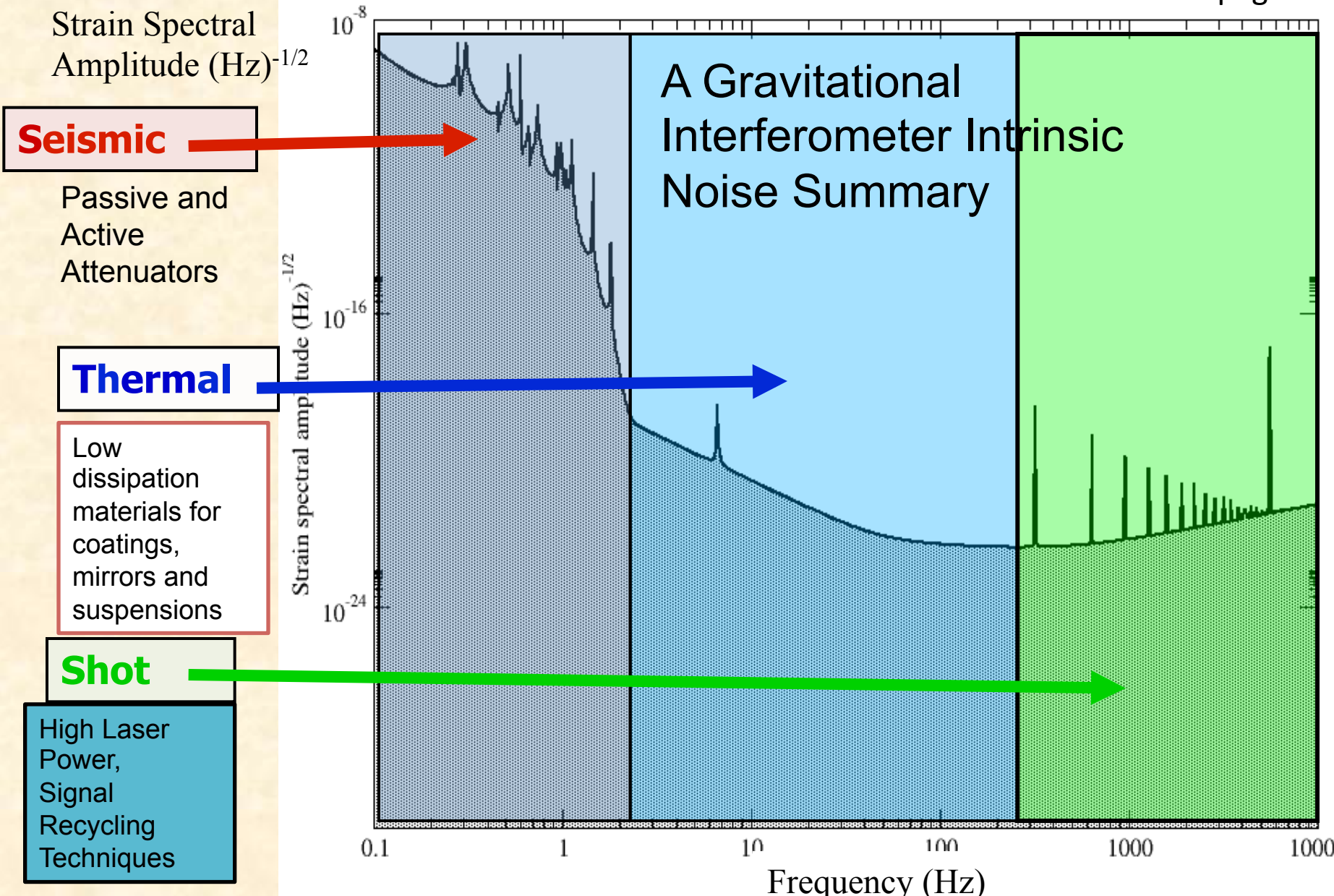
"Sapienza" – Jan 16th 2017

Network of the second generation of detectors



From first generation to Advanced Detectors: noise reduction

Credit: P. Rapagnani



AdV integration (a.k.a. “crossing the desert”)

▶ Started in 2013

▶ Reducing thermal noise:

- ▶ Increased beam size @ input TM (2.5 x larger)
- ▶ Larger Mirror Masses (2x larger, 42 kg instead of 21 kg)
- ▶ Improved mirrors' planarity (16 x better)
- ▶ Improved coatings for lower losses (7 x better)

→ Failure of monolithic suspensions under vacuum (finally fall back to steel wires to suspend mirrors)

▶ Reducing quantum noise:

- ▶ Increased finesse of arm cavities (3 x larger than Virgo+) than Virgo+)
- ▶ High power laser (16 x more input power)
- ▶ Heavier test masses (2 x heavier)

▶ Seismic isolation:

- ▶ iVirgo superattenuators compatible with AdV specs
- ▶ adapted for new payload (added mass and complexity)
- ▶ new electronics

▶ Thermal compensation (100 x higher power on TM):

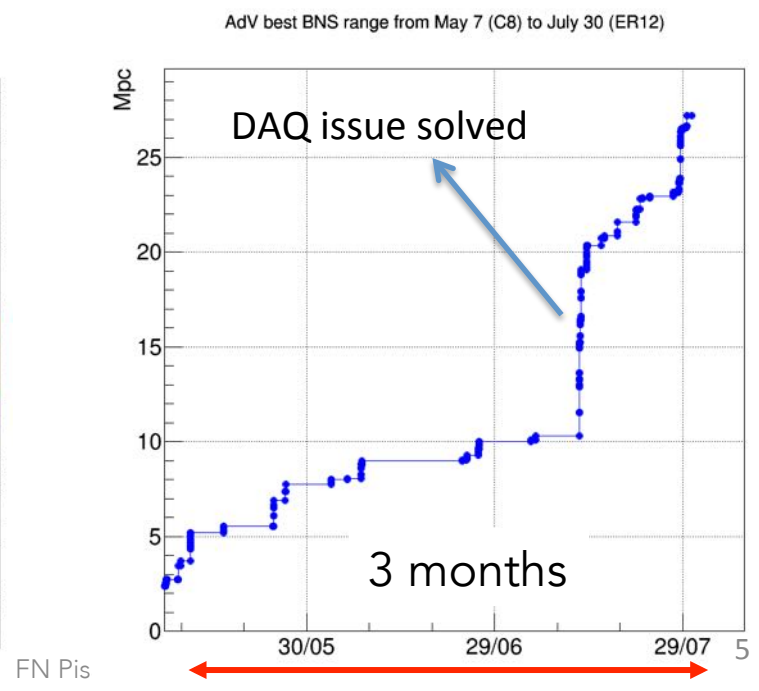
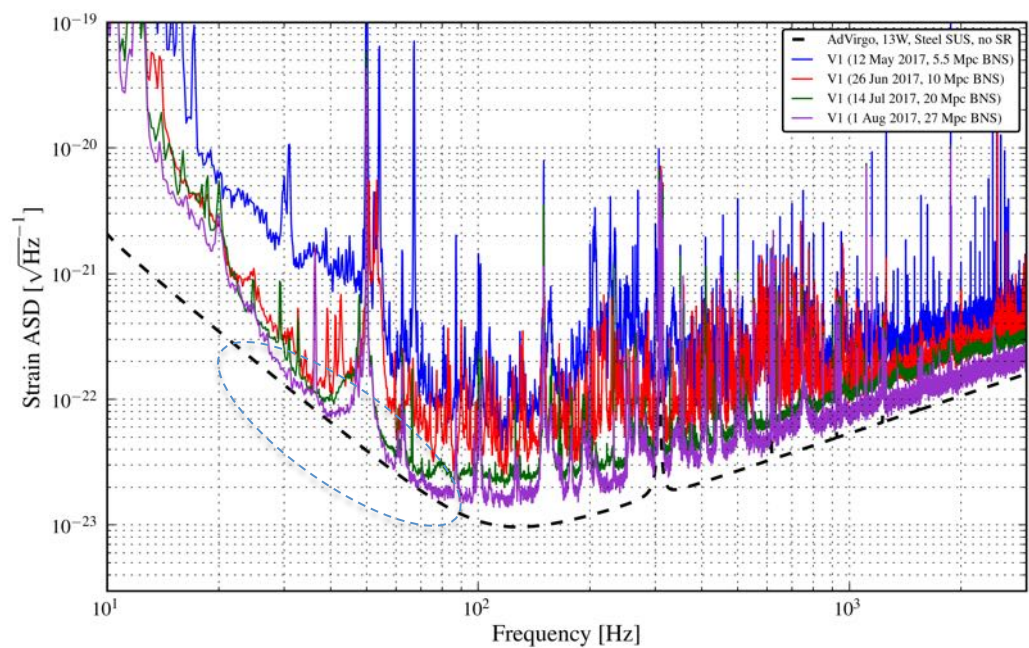
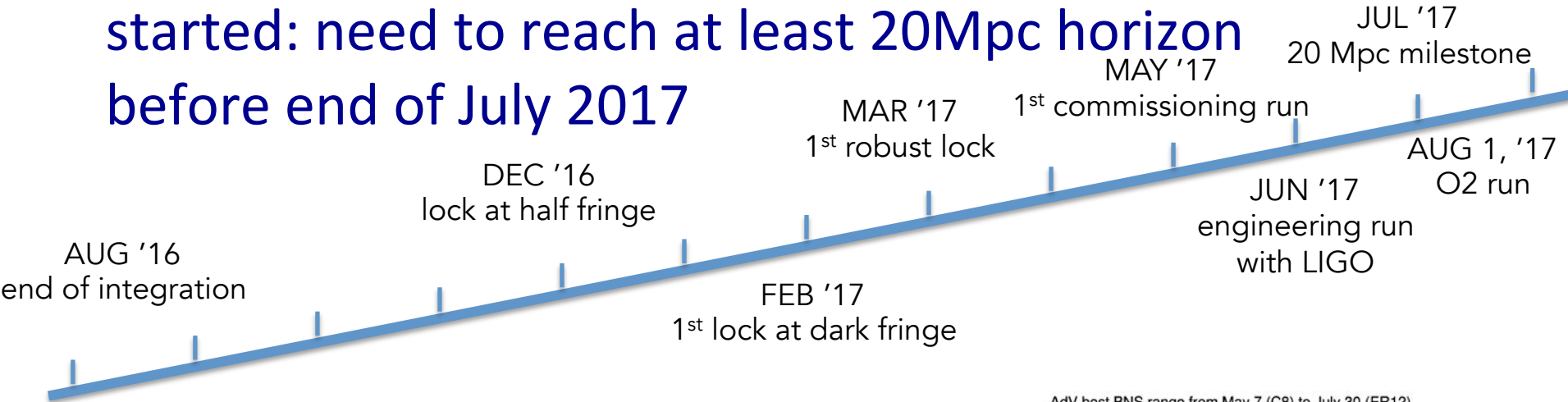
- ▶ ring heaters
- ▶ double axicon CO₂ actuators
- ▶ CO₂ central heating

▶ Better vacuum (10⁻⁹ mbar instead of 10⁻⁷)

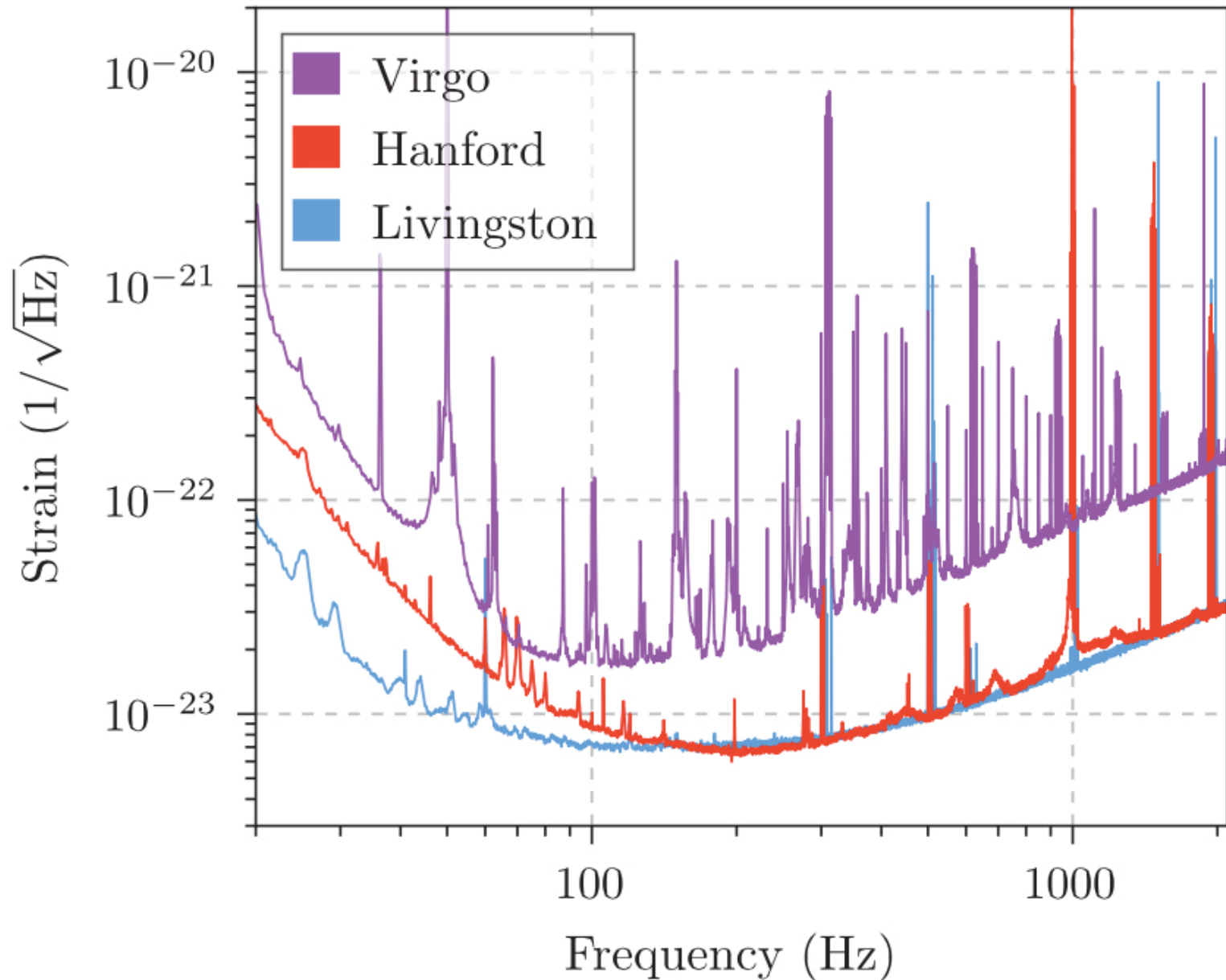
▶ Stray light control

- ▶ Suspended external optical benches in vacuum
- ▶ New set of baffles

- In August 2016 Advanced Virgo was completed and ...
- The Commissioning rush to join Advanced LIGO in run O2 started: need to reach at least 20Mpc horizon before end of July 2017

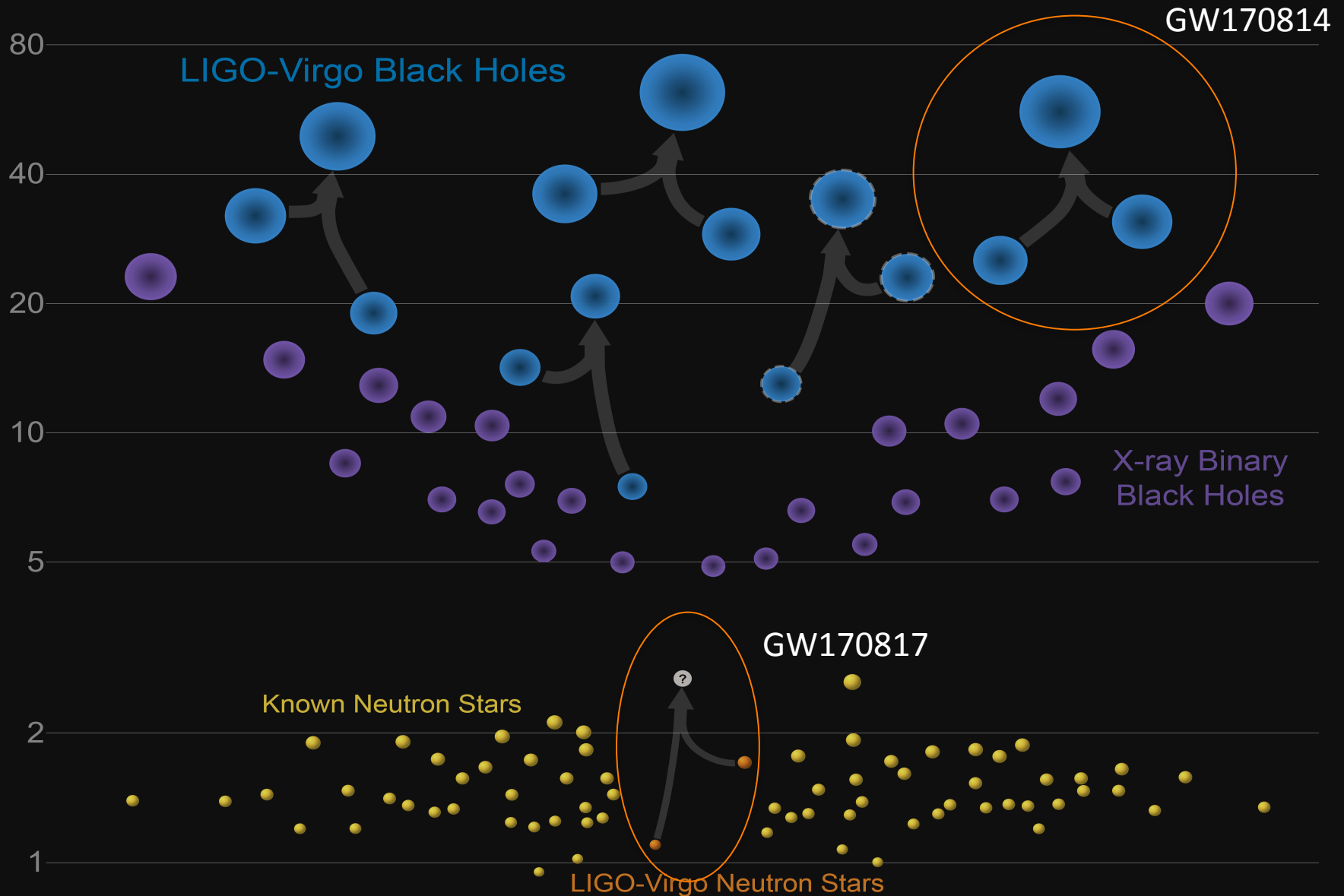


O2 noise amplitude spectral density



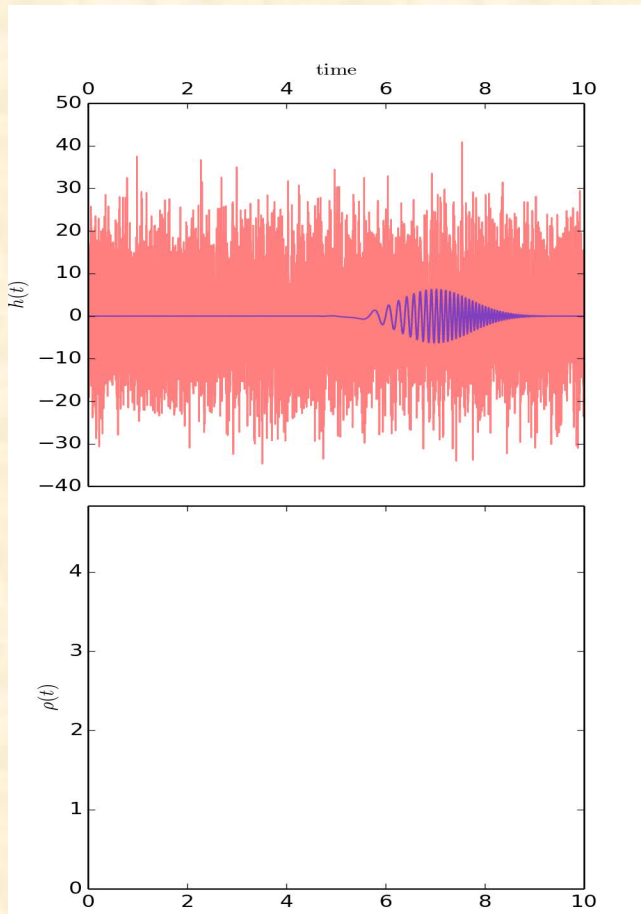
Masses in the Stellar Graveyard

in Solar Masses



How are the coalescing binary signals searched for

- To search a known signal in stationary and Gaussian noise the optimal strategy is based on matched filtering, which consists in correlating the data with the expected waveform



$$\hat{s} = \int K(t)s(t)dt$$

SNR maximization:

$$\rightarrow \tilde{K}(f) \propto \frac{\tilde{h}(f)}{S_n(f)} \rightarrow SNR = 2\sqrt{\int_0^{\infty} \frac{|\tilde{h}(f)|^2}{S_n(f)} df}$$

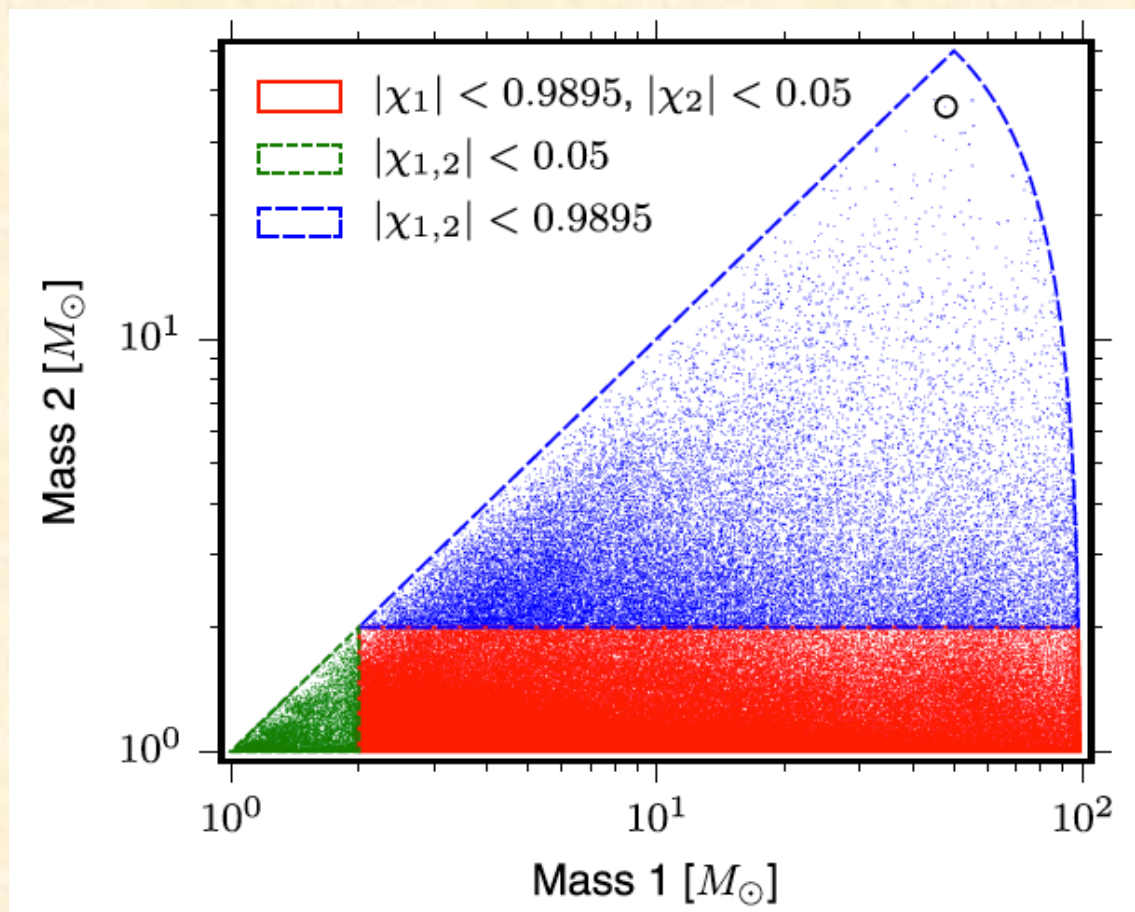
- Significant peaks in the filter output are searched for

In practice the signal phase and amplitude depend on several source parameters

- Early inspiral mainly driven by the chirp mass $\frac{(m_1 m_2)^{3/5}}{(m_1 + m_2)^{1/5}}$
- As the orbit shrinks: mass ratio $q = \frac{m_2}{m_1}$, spin $\chi_{1,2} = \left| \frac{c\mathbf{S}_{1,2}}{Gm_{1,2}^2} \right|$
- Also spin-orbit and spin-spin coupling affect system evolution
- Tidal polarizability if at least one NS is present

- Use a template bank to properly cover the parameter space
- $O(10^5)$ templates for a typical search

Template bank for GW150914



- Detector noise is not perfectly described by a stationary Gaussian process
 - Data gating and quality vetoes to remove noise transients and instrumental disturbances
 - χ^2 – signal consistency test on triggers to check if the time-frequency distribution of the power in the data is consistent with the power in the matching template

$$\chi_r^2 = \frac{p}{2p-2} \frac{1}{\langle h|h \rangle} \sum_{i=1}^p \left| \langle s|h_i \rangle - \frac{\langle s|h \rangle}{p} \right|^2$$

p: number of frequency bands
 h_i : sub-template corresponding to ith band

$\chi_r^2 \sim 1$ for real signals

→ re-weighted SNR

$$\hat{\rho} = \begin{cases} \rho / [(1 + (\chi_r^2)^3)/2]^{\frac{1}{6}}, & \text{if } \chi_r^2 > 1 \\ \rho, & \text{if } \chi_r^2 \leq 1 \end{cases}$$

- Clustering and selection of single-detector triggers

- Coincidence among detectors
 - same trigger template in all the detectors
 - arrival time compatible with signal propagation
- Candidate events are ranked according to $\rho_c = \sqrt{\sum_i \hat{\rho}_i^2}$
- Candidate significance based on false alarm (empirically measured)
 - background data set produce by time shifting triggers in one detector with respect to the other detectors

$$p(\geq 1 \text{ above } \hat{\rho}_c^* | T, T_b)_0 = 1 - \exp \left[\frac{-T(1 + n_b(\hat{\rho}_c^*))}{T_b} \right]$$

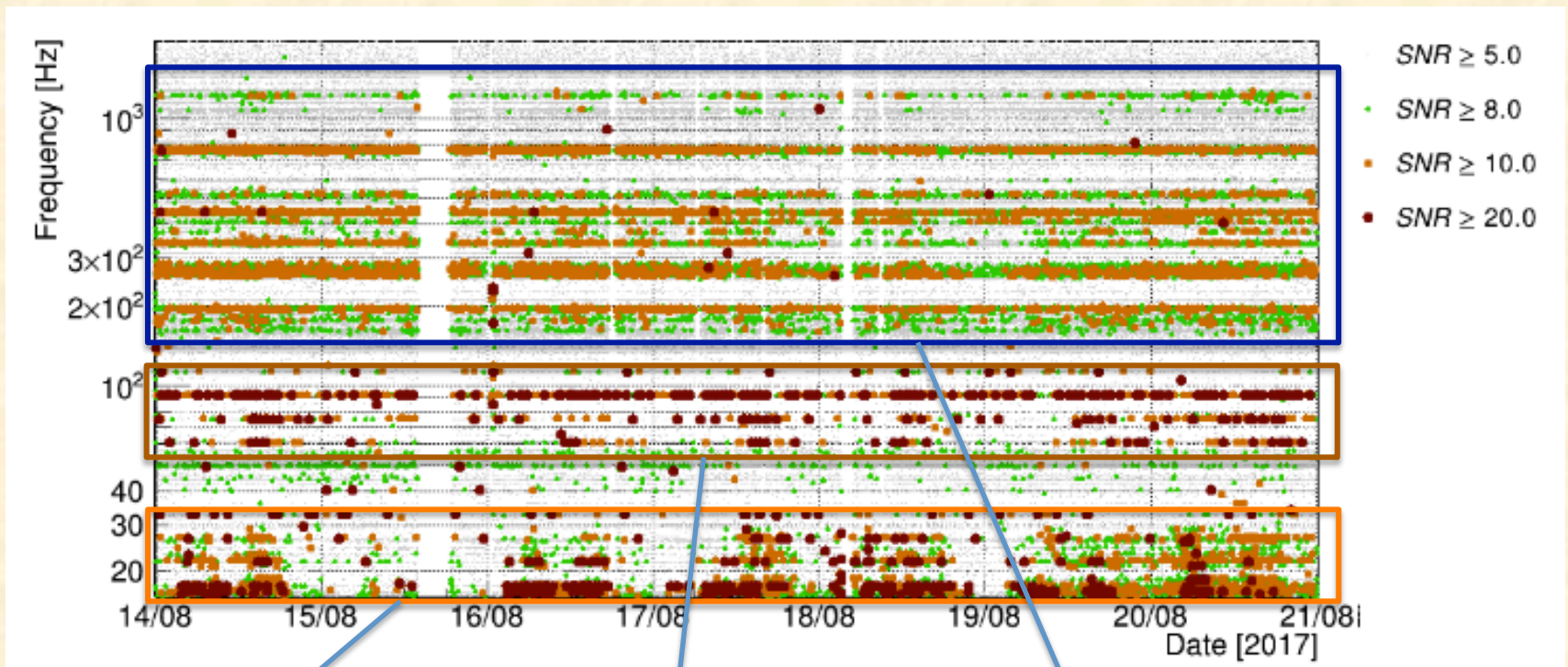
Probability of having at least one noise event with detection statistic higher than what obtained in the analysis (from Poisson statistic).

T: observing time

T_b : background time

n_b : number of noise events > threshold

Glitch time-frequency distribution in the period 14-21/08/2017 (Virgo O2)

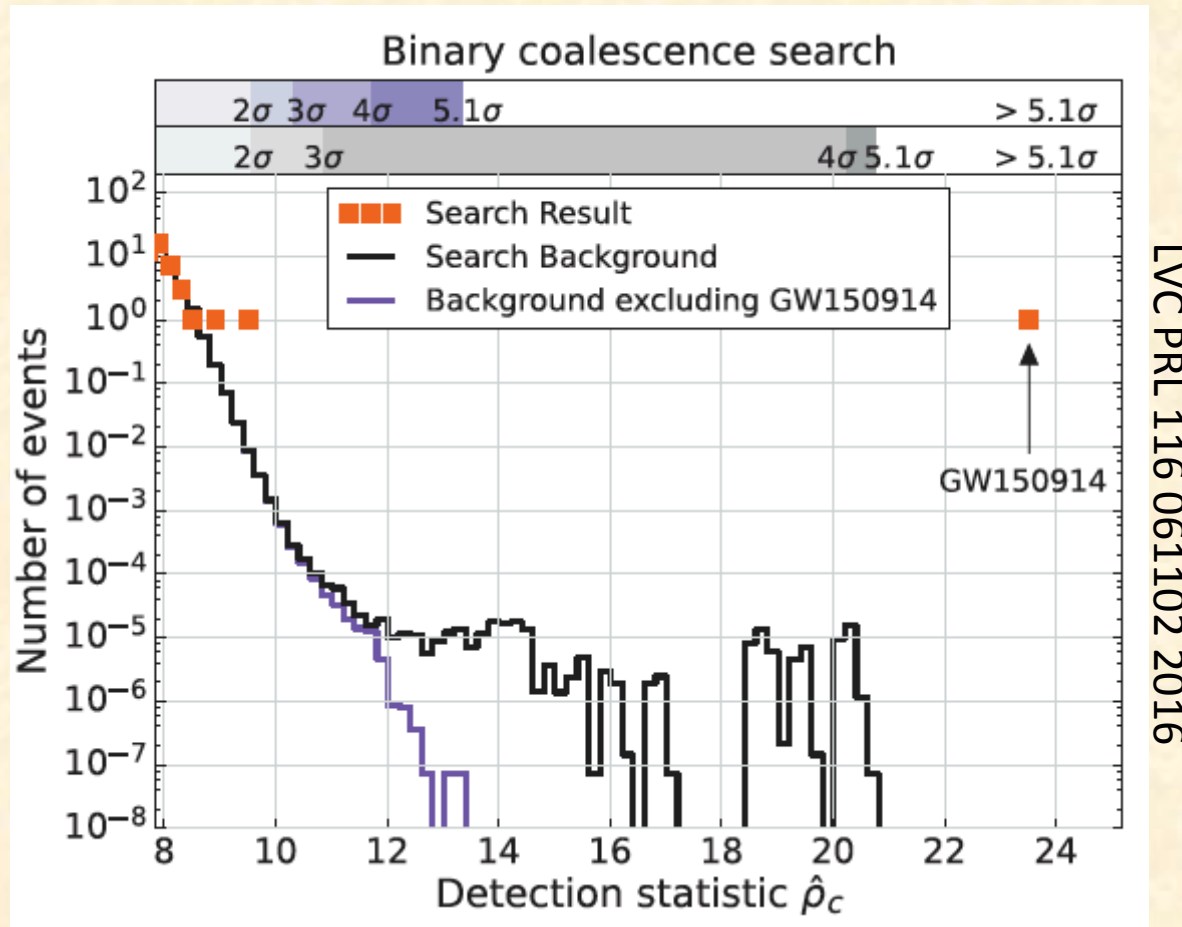


Microseismic activity

Missing samples in
control loops

Scattered light

An example: significance estimation for GW150914



- $FAR = p/T$
- Significance in terms of Gaussian std: $-\sqrt{2}\text{erf}^{-1}[1 - 2(1 - p)]$

- Parameter estimation often based on Bayesian inference

$$p(\theta|d, H) = \frac{p(\theta|H)p(d|\theta, H)}{p(d|H)}$$

prior

Likelihood
(waveforms enter here)

Joint posterior distribution of
parameter vector $\vartheta = [\vartheta_1, \vartheta_2, \dots, \vartheta_n]$

marginal likelihood

- Results for a single parameter by marginalization:

$$p(\theta_1|d, H) = \int d\theta_2 \dots d\theta_N p(\theta|d, H)$$

- Calibration errors straightforward to be included
- credible intervals, mean value, etc.

- Model comparison by means of odds ratios

$$O_{ij} = \frac{P(H_i|d)}{P(H_j|d)}$$

proportional to the Bayes factor

Transient source localization

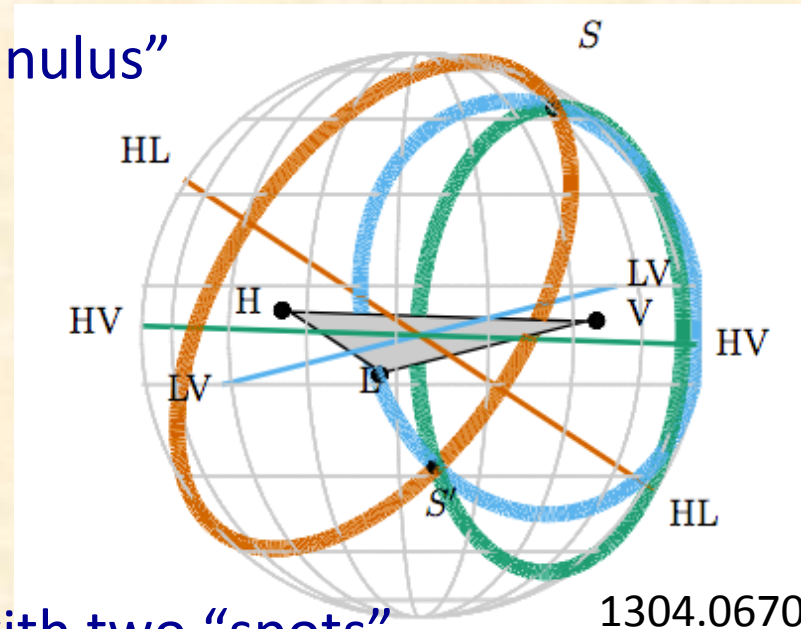
- Triangulation using signal time delays among sites

- With two detectors there is an “annulus” of possible locations

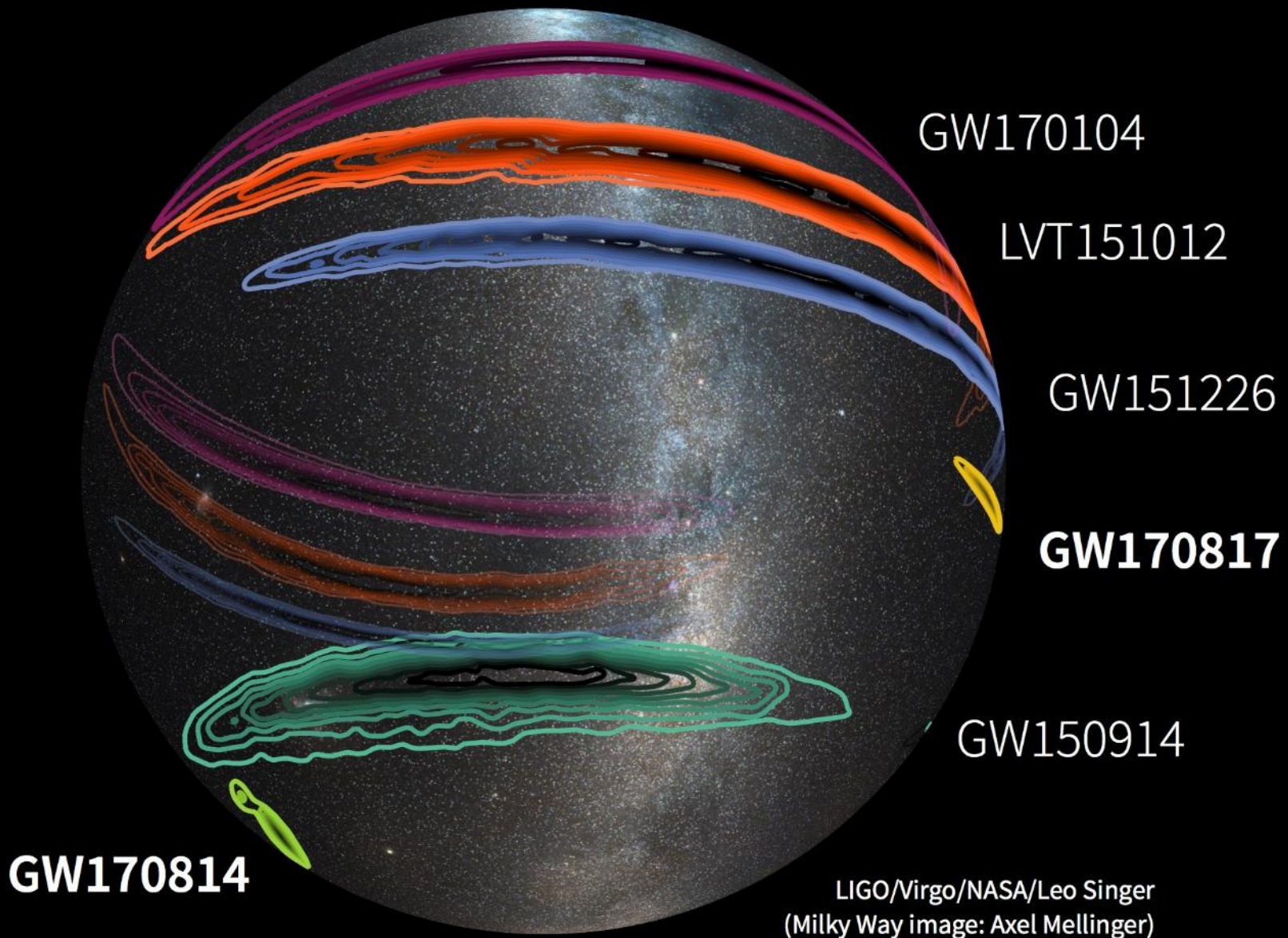
- Width related to the event timing accuracy, proportional to SNR

$$\sigma_t \approx 100 \left(\frac{\rho}{10} \right)^{-1} \mu s$$

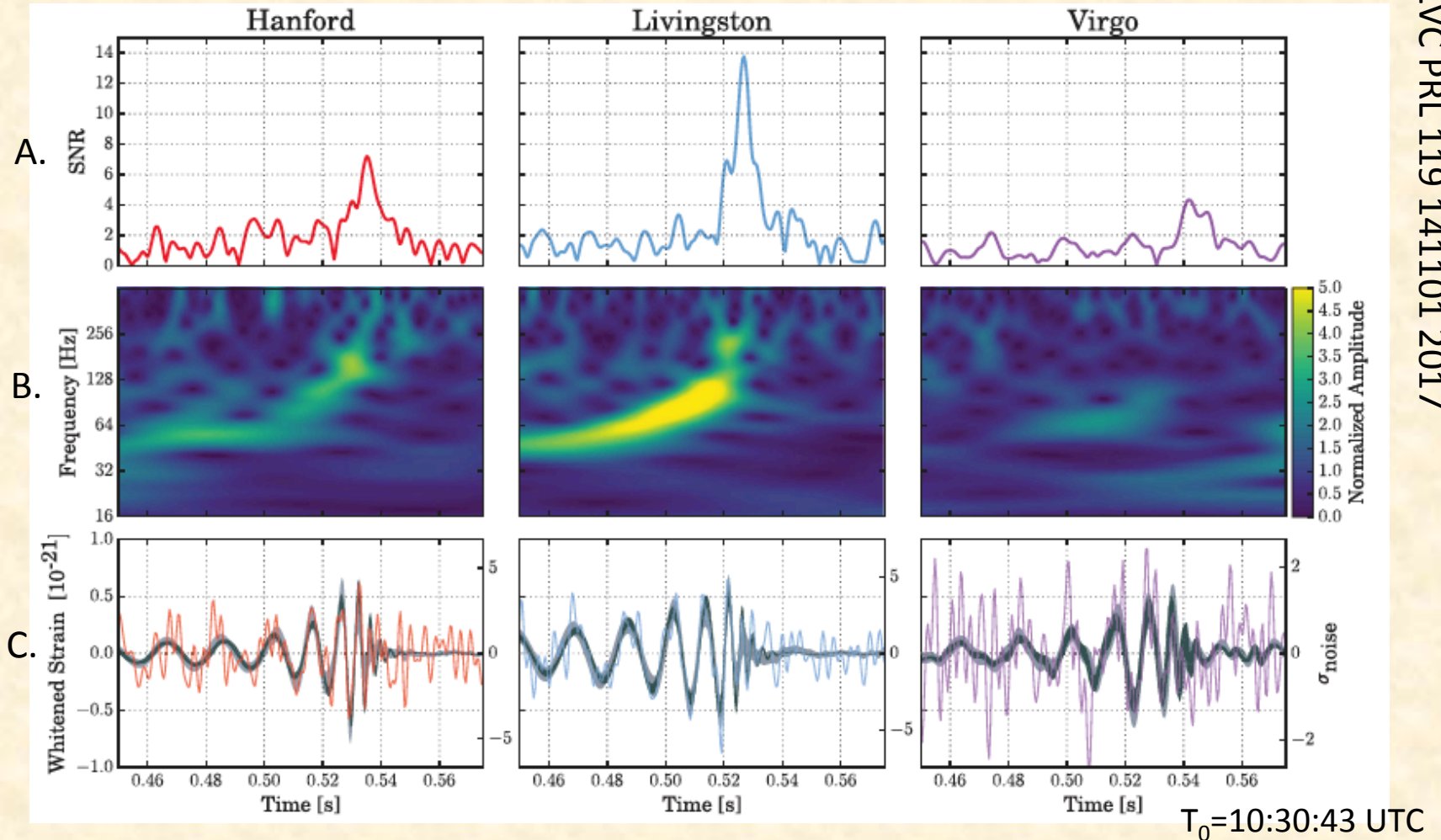
- With three detectors we are left with two “spots”



- Localization improved using signal phase and amplitude information
- Having a relatively small error box crucial for EM-followup



GW170814 BBH coalescence



A.: Matched filter signal-to-noise ratio vs. time (low-latency search)

B. Time-frequency representation

C. Time-domain data and reconstructed waveforms (withened, low-passed)

- First identified in all three detectors by two independent low-latency matched filter pipelines
 - Use approximate templates
 - Provide alert (within minutes) to EM partners for rapid follow-up
- Confirmed by off-line analyses, including a coherent unmodeled search, with FAR < 1/140,000 years
- Single detector matched filter: 9.7, 14.8, 4.8 → $\rho_c=18.3$

Impact of Virgo on the detection

- 0.3% probability of a random SNR peak in Virgo data compatible with what observed
 - Un-modeled search shows an improvement of a factor $O(10)$ in the FAR by including Virgo w.r.t. the LIGO network alone
 - The three detector BBH signal model preferred with a Bayes factor of 1600 w.r.t. a model with BBH signal in LIGO detectors + Gaussian noise in Virgo
 - Relative SNRs in agreement with detector sensitivities
- Virgo has clearly detected this signal

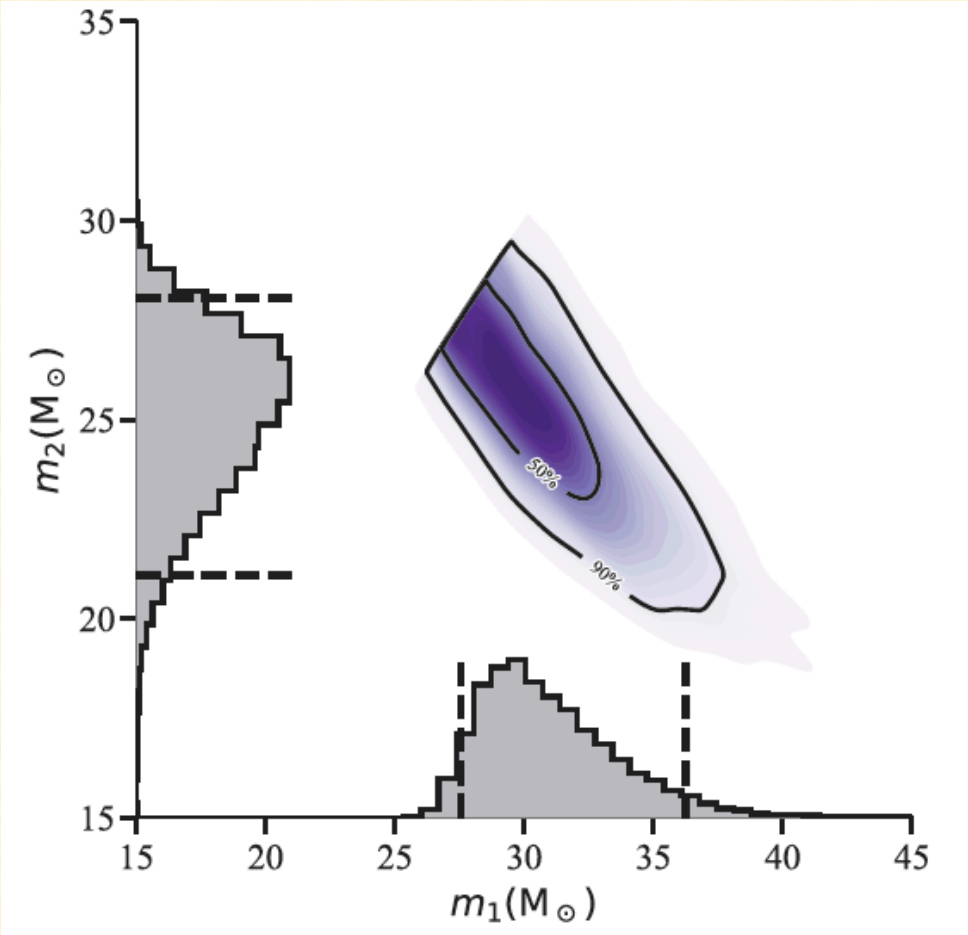
GW170814 parameters (median with 90% credible interval)

| | | |
|---|---|---------------------|
| Primary black hole mass m_1 | $30.5_{-3.0}^{+5.7} M_{\odot}$ | |
| Secondary black hole mass m_2 | $25.3_{-4.2}^{+2.8} M_{\odot}$ | |
| Chirp mass \mathcal{M} | $24.1_{-1.1}^{+1.4} M_{\odot}$ | binary inspiral |
| Total mass M | $55.9_{-2.7}^{+3.4} M_{\odot}$ | merger and ringdown |
| Final black hole mass M_f | $53.2_{-2.5}^{+3.2} M_{\odot}$ | |
| Radiated energy E_{rad} | $2.7_{-0.3}^{+0.4} M_{\odot} c^2$ | fit to NR waveforms |
| Peak luminosity ℓ_{peak} | $3.7_{-0.5}^{+0.5} \times 10^{56} \text{ erg s}^{-1}$ | |
| Effective inspiral spin parameter χ_{eff} | $0.06_{-0.12}^{+0.12}$ | binary inspiral |
| Final black hole spin a_f | $0.70_{-0.05}^{+0.07}$ | Fit to NR waveform |
| Luminosity distance D_L | $540_{-210}^{+130} \text{ Mpc}$ | |
| Source redshift z | $0.11_{-0.04}^{+0.03}$ | |

$$z \cong \frac{H_0}{c} D_L$$

- Bayesian procedure using two independent waveform models (calibrated to NR simulations)

Posterior probability density for the source-frame masses



GW170814 localization

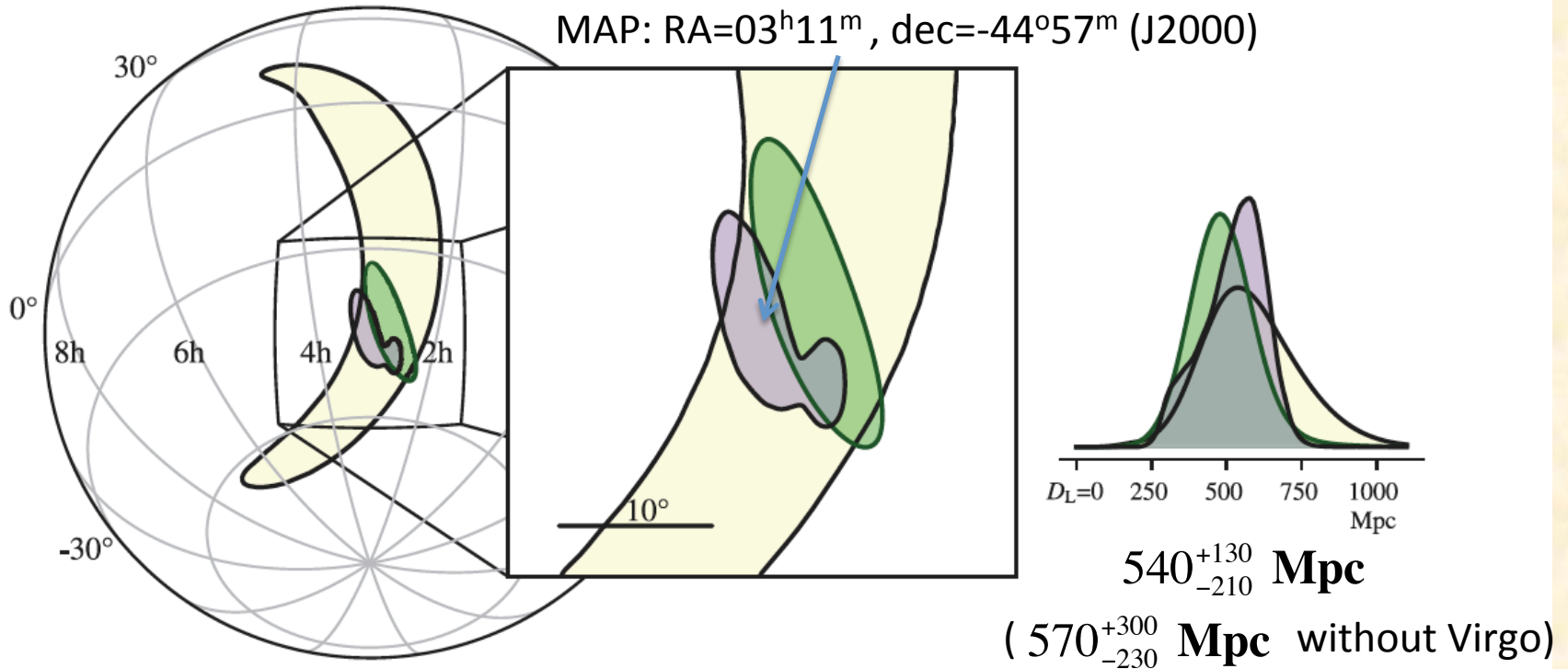


FIG. 3. Localization of GW170814. The rapid localization using data from the two LIGO sites is shown in yellow, with the inclusion of data from Virgo shown in green. The full Bayesian localization is shown in purple. The contours represent the 90% credible regions. The left panel is an orthographic projection and the inset in the center is a gnomonic projection; both are in equatorial coordinates. The inset on the right shows the posterior probability distribution for the luminosity distance, marginalized over the whole sky.

HLV rapid localization 90% credible area: 100 deg² (1160 deg² HL alone)

Refined parameter estimation: 60 deg² centered at the MAP

3D credible volume: 2.1E6 Mpc³ (initially 71E6 Mpc³ without Virgo)

→ from thousands to few tens of target galaxies

GW polarization studies

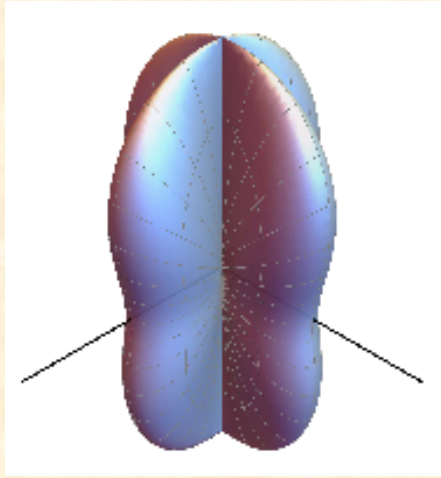
- The two LIGO detectors are nearly co-aligned. This prevents from measuring the polarization content for transient GW signals
- By adding Virgo polarization can be studied by projecting the metric perturbation on the detector network (5 not aligned detectors would be needed to break all the degeneracies)

$$h_I(t) = D_I^{ab} h_{ab}(t, \mathbf{x}_I) = h_A(t, \mathbf{x}_I) D_I^{ab} e_{ab}^A$$

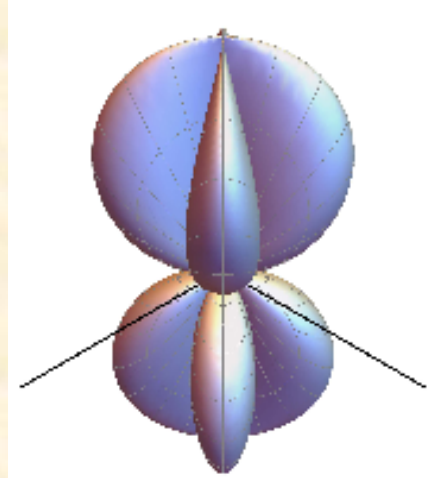
The diagram illustrates the decomposition of the detector tensor D_I^{ab} into a polarization tensor e_{ab}^A and a detector angular response. The term $D_I^{ab} e_{ab}^A$ in the equation is circled in orange. Three blue arrows originate from this circled term: one points to the label "detector tensor" above, one points to the label "polarization tensor" to the right, and one points to the label "detector angular response" below.

Angular response of a quadrupolar detector

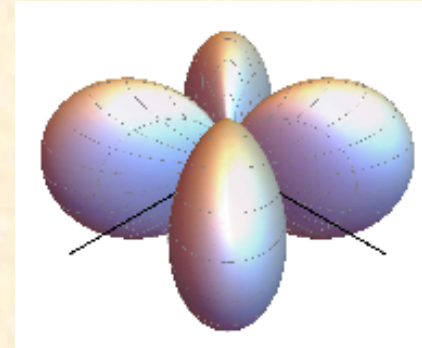
C. deRham, Living
Reviews of Rel. 17 2014



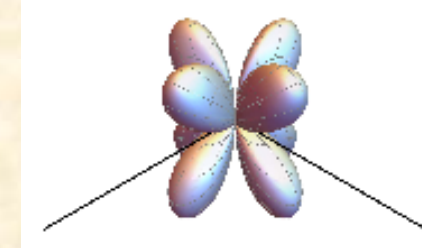
Tensor +



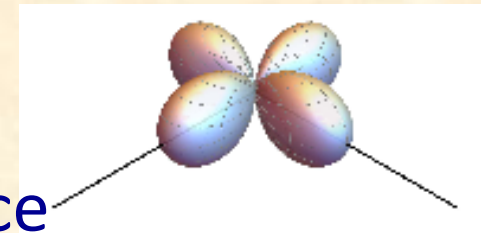
Tensor x



Vector-x



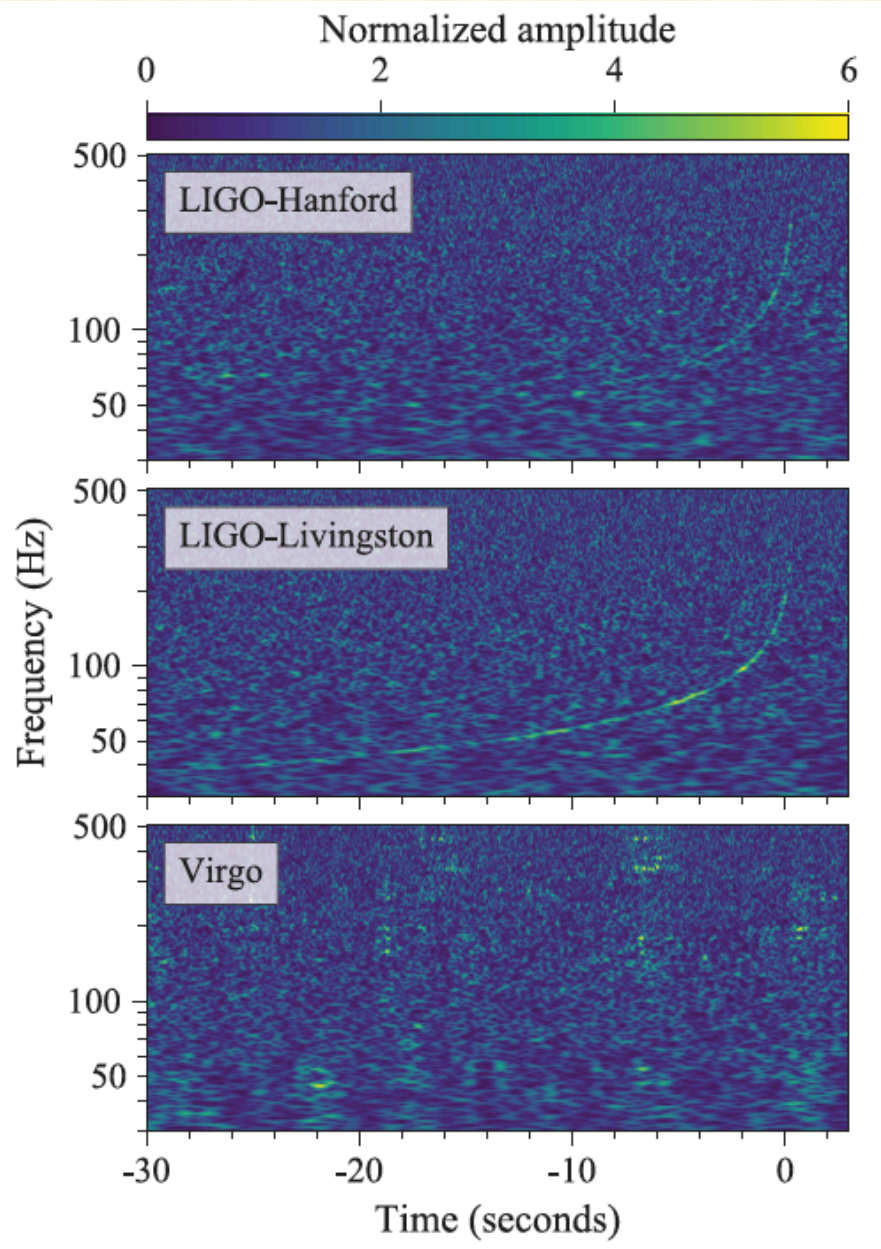
Vector-y



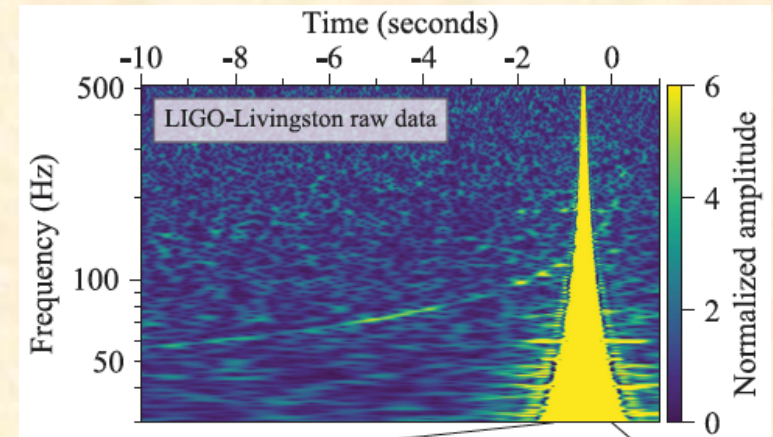
Scalar (breathing
and longitudinal)

- Preliminary analysis shows large preference for pure tensor w.r.t. pure vector or pure scalar ($B > 200$ and 1000)
- Need to consider mixed polarization states
- Continuous GW signals will allow much more accurate studies

GW170817: BNS coalescence

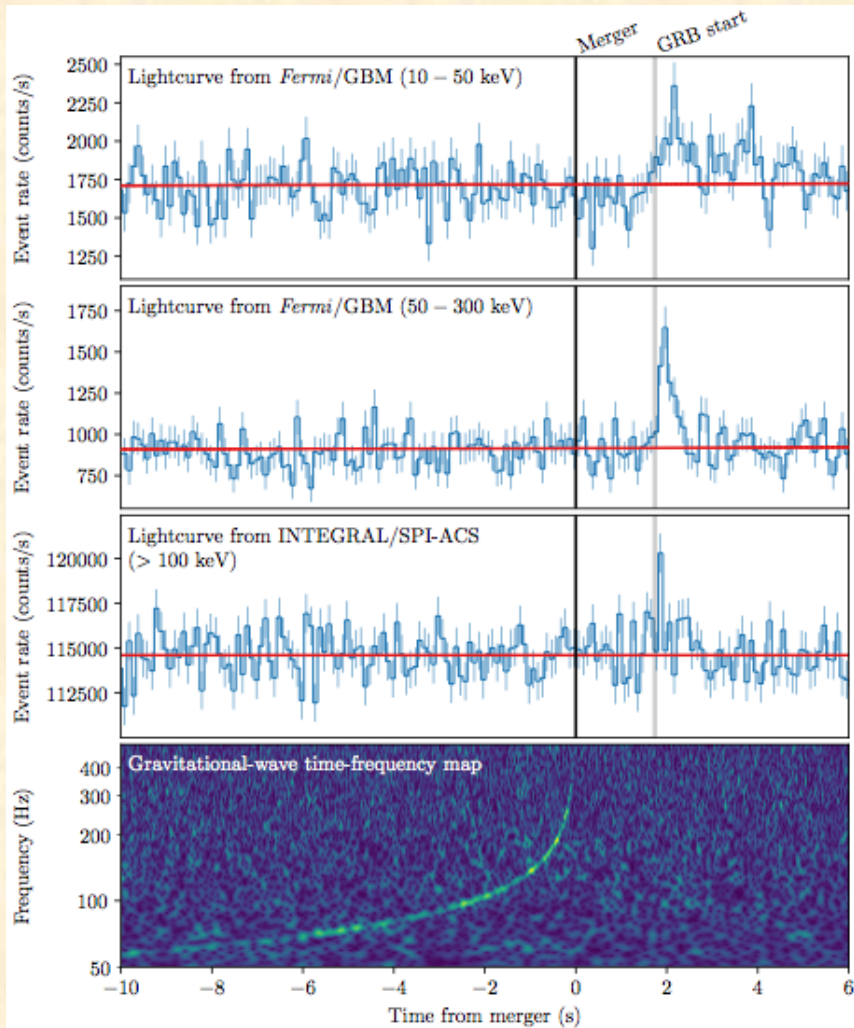


- First identified on-line in LIGO-H (LIGO-L affected by a glitch, Virgo had bad orientation)



- SNR: 18.8, 26.4, 2.0 (32.4 combined)
- ~60 seconds from 30 Hz to coalescence
- FAR~1/1.1E6 years

- Followed by a Fermi/Integral GRB trigger 1.7 s later (but Fermi circulated the alert before)
- Demonstration that at least some short GRB are due to the coalescence of BNS



Estimated parameters (source frame) – 90% posterior prob. intervals

| | Low-spin priors ($ \chi \leq 0.05$) | High-spin priors ($ \chi \leq 0.89$) |
|--|--|---|
| Primary mass m_1 | 1.36–1.60 M_\odot | 1.36–2.26 M_\odot |
| Secondary mass m_2 | 1.17–1.36 M_\odot | 0.86–1.36 M_\odot |
| Chirp mass \mathcal{M} | 1.188 $^{+0.004}_{-0.002}$ M_\odot | 1.188 $^{+0.004}_{-0.002}$ M_\odot |
| Mass ratio m_2/m_1 | 0.7–1.0 | 0.4–1.0 |
| Total mass m_{tot} | 2.74 $^{+0.04}_{-0.01}$ M_\odot | 2.82 $^{+0.47}_{-0.09}$ M_\odot |
| Radiated energy E_{rad} | $> 0.025 M_\odot c^2$ | $> 0.025 M_\odot c^2$ |
| Luminosity distance D_L | 40 $^{+8}_{-14}$ Mpc | 40 $^{+8}_{-14}$ Mpc |
| Viewing angle Θ | $\leq 55^\circ$ | $\leq 56^\circ$ |
| Using NGC 4993 location | $\leq 28^\circ$ | $\leq 28^\circ$ |
| Combined dimensionless tidal deformability $\tilde{\Lambda}$ | ≤ 800 | ≤ 700 |
| Dimensionless tidal deformability $\Lambda(1.4M_\odot)$ | ≤ 800 | ≤ 1400 |

very accurate thanks to the very long chirp (~3000 cycles)

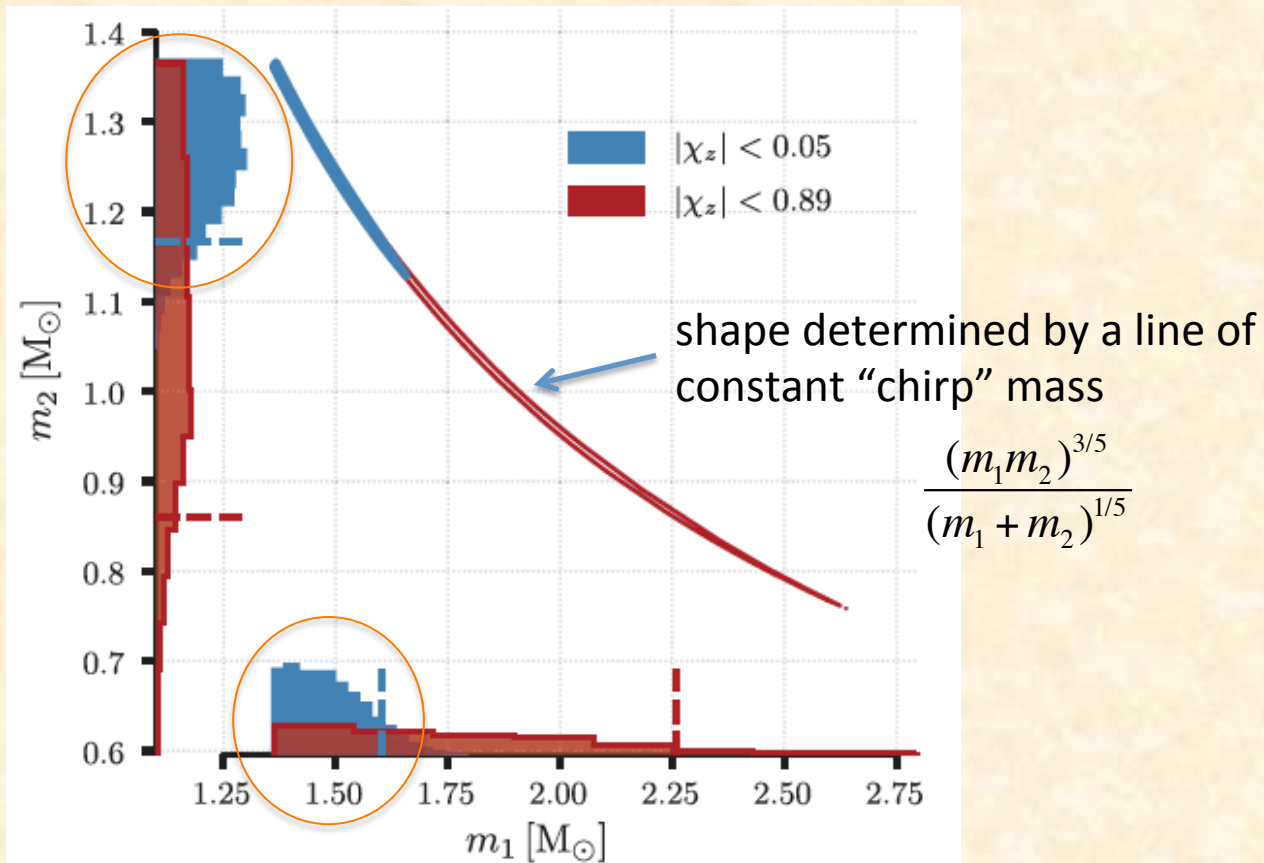
Not enough SNR at frequency above 500 Hz, where tidal effects start to be important

Using an independent distance measure improves viewing angle measure

nearest GRB ever

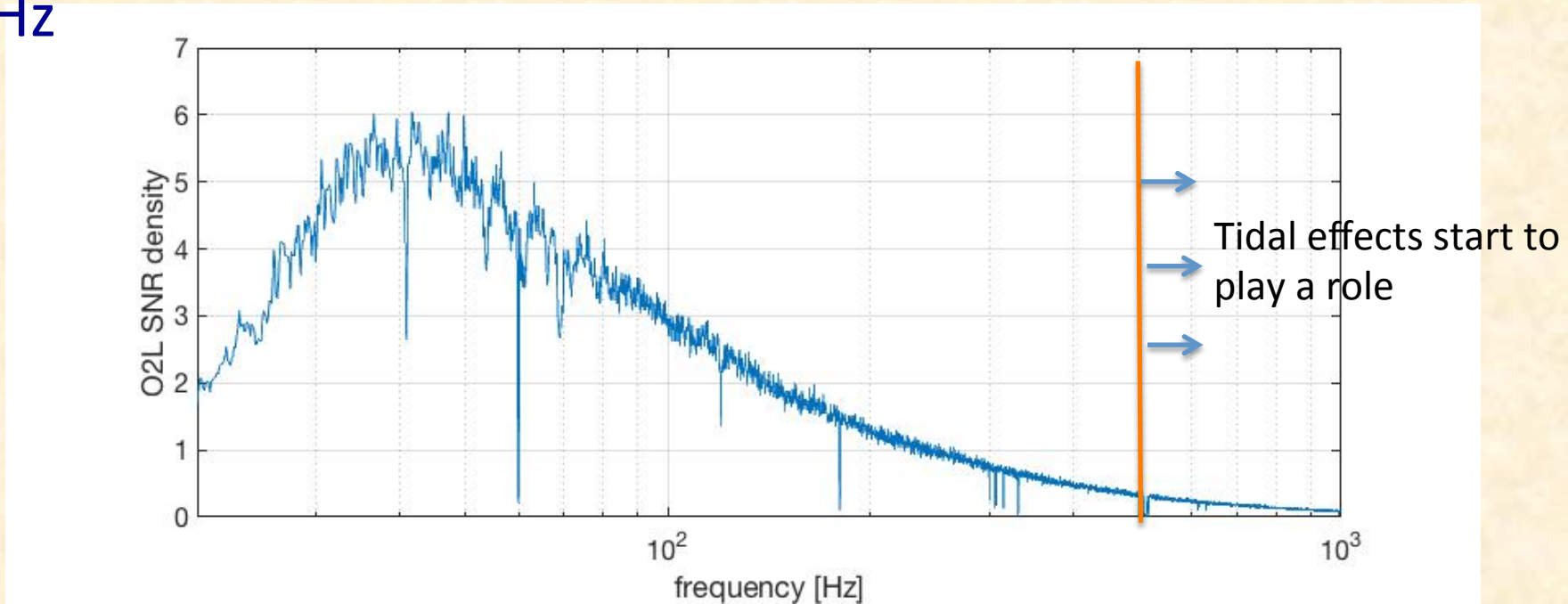
- Virgo contribution negligible for parameter estimation, but crucial for localization

Posterior probability distribution for NS masses



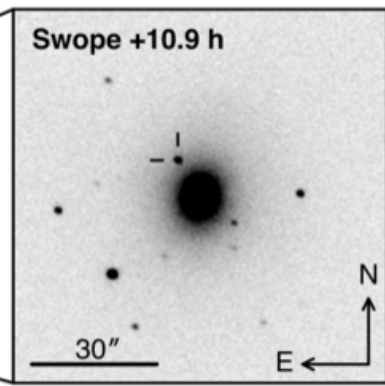
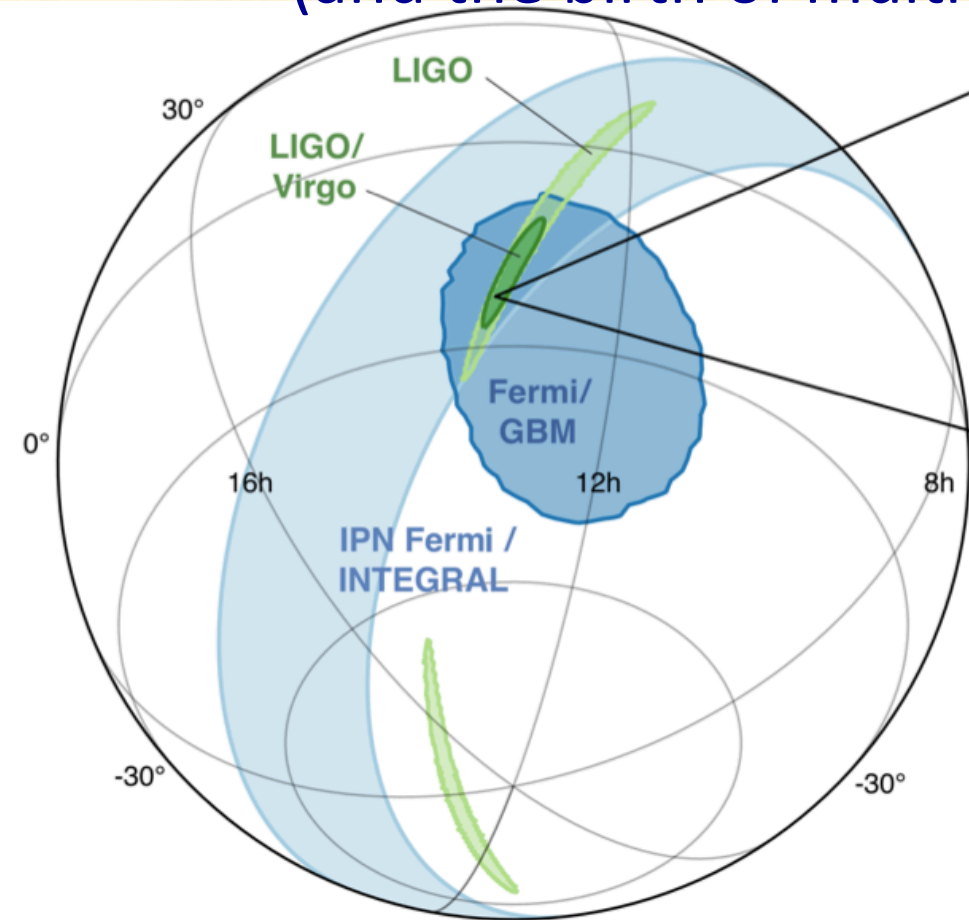
- Single masses estimation are affected by degeneracy between mass ratio q and aligned spin component $\chi_{i,z}$
- Assuming low-spin prior the masses are better constrained and consistent with those of known binary neutron star systems

- Most of the SNR is accumulated at frequency below ~ 200 Hz



- Better high frequency sensitivity needed + better waveform models

GW170817 sky localization (and the birth of multi-messenger astronomy)

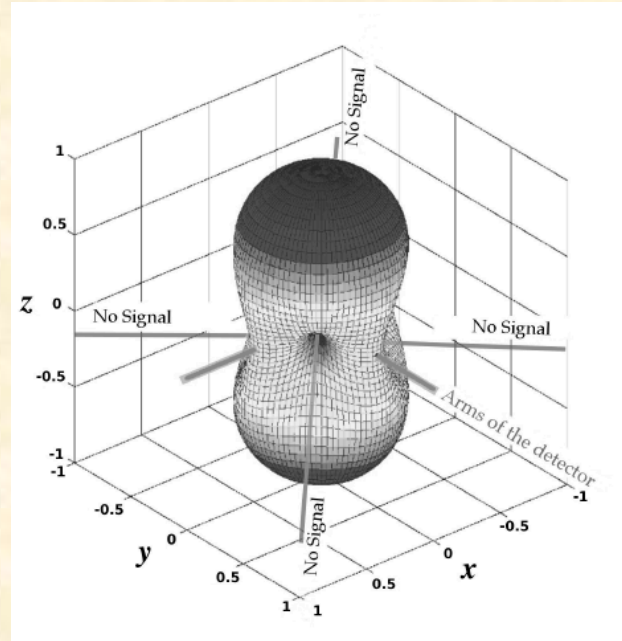


*Location of the apparent host **galaxy NGC 4993** in the **Swope optical discovery image** (10.9 h after the merger)*

Approximately 100 ground- and space- based observatories followed-up on this event

- $190 \text{ deg}^2 \rightarrow 28 \text{ deg}^2$ thanks to Virgo detector
- But, most of all, shift in the maximum of the posterior

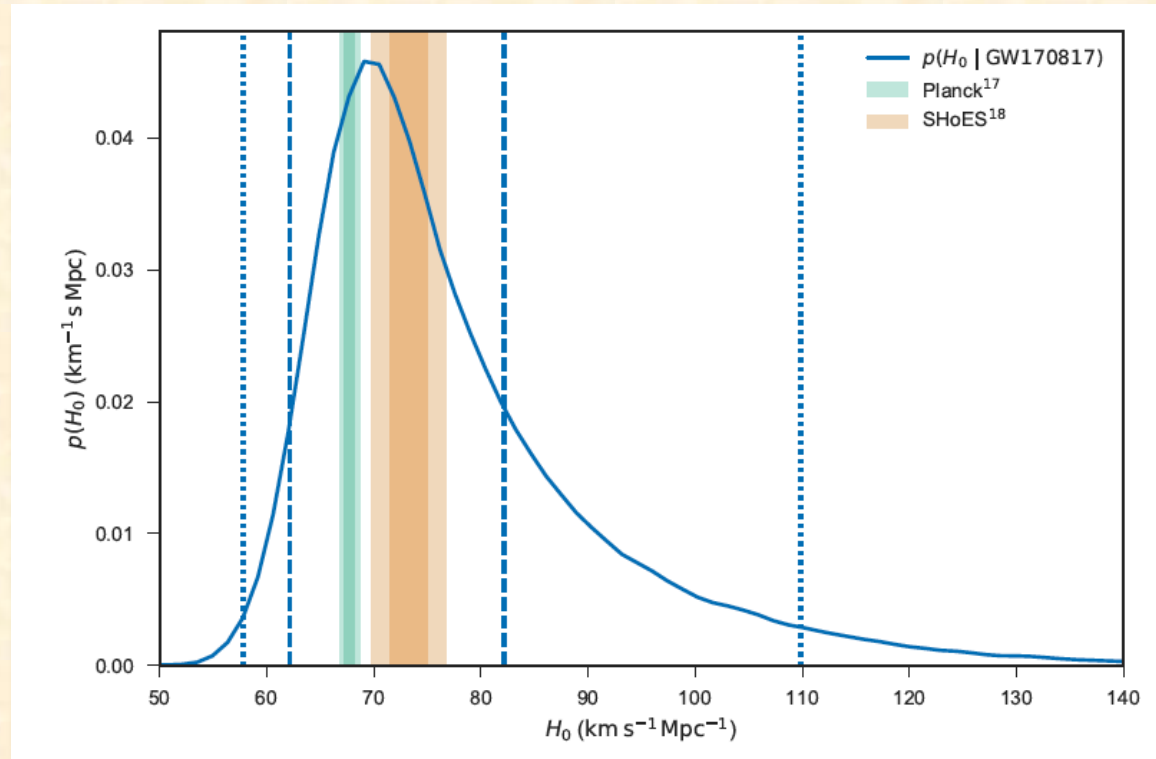
- Source position at the blind spot of Virgo



- Response reduced by ~ 3 w.r.t. LIGO detectors
- Blind spot is very localized, this helped in source localization

Multi-messenger astronomy: an example


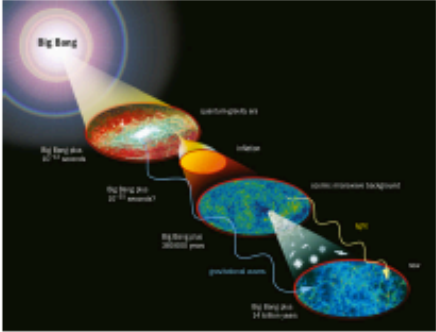
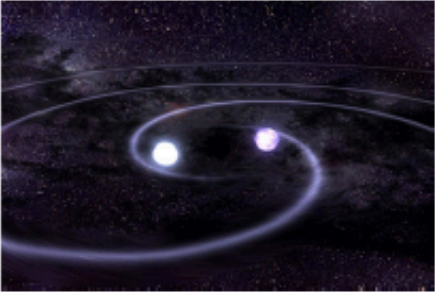
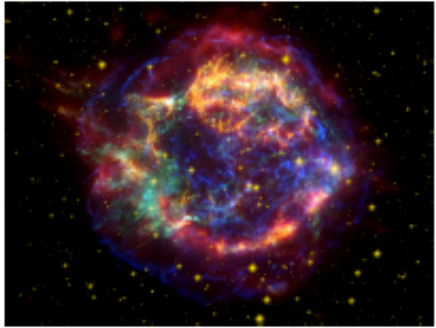
$$H_0 = 70.0^{+12.0}_{-8.0} \text{ km s}^{-1} \text{ Mpc}^{-1}$$



Nature 551 85 2017

Not only coalescing compact binary systems

Credit: O. J. Piccinni

| | Modeled waveform | Unknown waveform |
|------------|---|--|
| Long-lived |  |  |
| Transients |  |  |

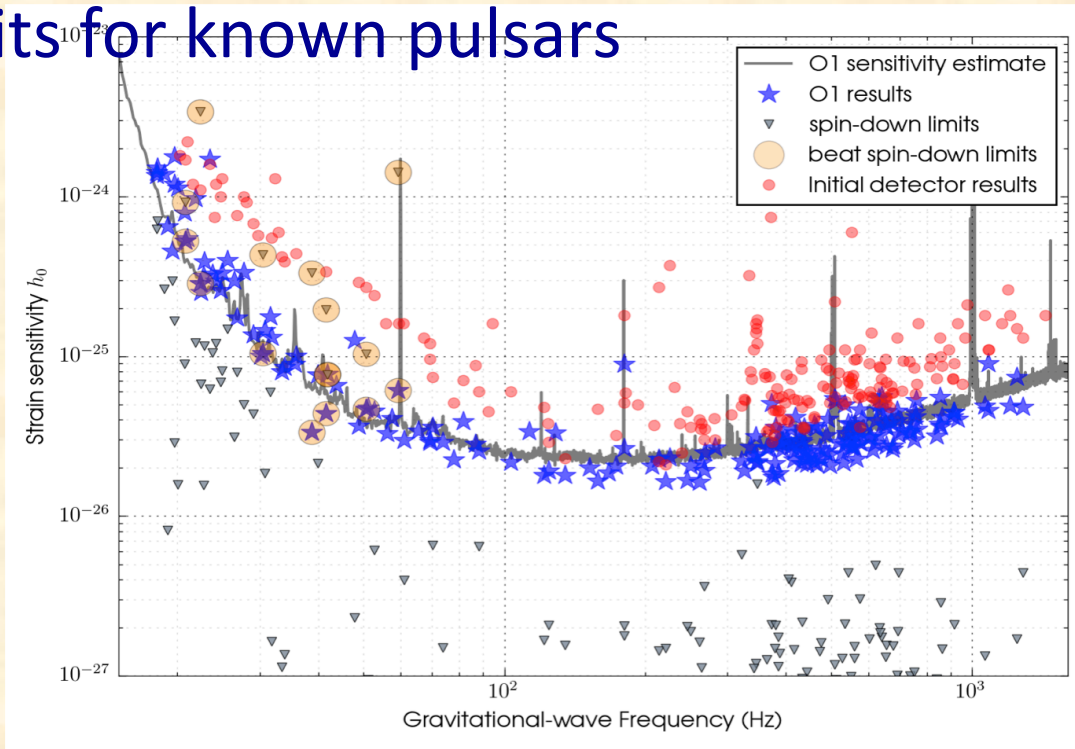
- Detection of “new” sources could be behind the corner

- For instance, neutron stars asymmetric w.r.t. the rotation axis emit a continuous GW signal

$$h_0 \cong 10^{-27} \left(\frac{I_{zz}}{10^{38} \text{ kg} \cdot \text{m}^2} \right) \left(\frac{10 \text{ kpc}}{d} \right) \left(\frac{f}{100 \text{ Hz}} \right)^2 \left(\frac{\varepsilon}{10^{-6}} \right)$$

- The ellipticity ε is largely unknown; $\sim 10^{-6}$ maximum expected for standard NSs, but for some exotic EOS could be 10^{-4} or even more.
- Deformation mechanisms include:
 - deformation due to elastic stresses or magnetic field (in isolated or in accreting NS due to the accretion process);
 - free precession around rotation axis;
 - excitation of long-lasting oscillations (e.g. r-modes); ...

O1 upper limits for known pulsars



LVC Apr 839 12 2017

- For pulsar Crab it implies a constraint of $\sim 2/1000$ on the fraction of rotational energy lost to GWs ($\epsilon < 3 \cdot 10^{-5}$)
- For such kind of sources signal parameters will be measured with extreme accuracy (thanks to signal long duration)
- Excellent tools to measure tiny effects that build-up in time

Short term plan

Credit: P. Rapagnani

Fall 2018 ==> start of O3 with 3 detectors in operation

Main improvements

LIGO

- mirror cleaning
- increased light power
- squeezed light in one interferometer
- vacuum leak repaired

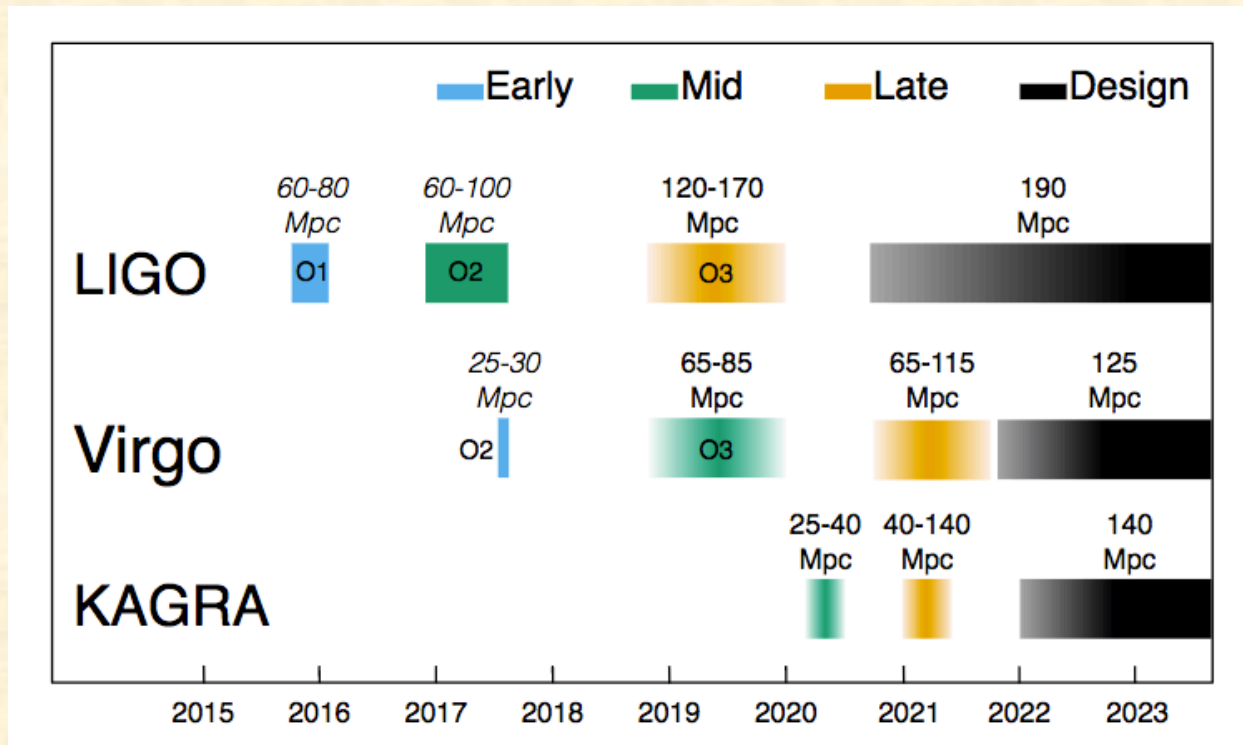
Virgo

- vacuum cleaning
- mirror cleaning
- monolithic suspension**
- electronics improvement
- new powerful laser
- frequency independent squeezing
- sensor deployment to test the Newtonian noise cancellation

Data taking duration ~ 1/(1.5?) year



Advanced +



LISA

3rd generation
(ET)